

## COMMUNICATION

[View Article Online](#)  
[View Journal](#) | [View Issue](#)



Cite this: *Environ. Sci.: Processes Impacts*, 2025, 27, 3076

Received 9th July 2025  
Accepted 31st July 2025

DOI: 10.1039/d5em00529a

rsc.li/espi

## Influence of microplastic colour on photodegradation of sorbed contaminants

Laura C. Matchett and Sarah A. Styler \*

Microplastics are ubiquitous in the environment, accumulate hydrophobic organic contaminants, and suppress the photodegradative loss of these contaminants. Thus, they have the potential to act as vectors for contaminant uptake by organisms and transport to remote regions. Our current understanding of microplastic-sorbed contaminant photodegradation is drawn from experiments with unpigmented microplastics, but the interaction of pigments with light may alter the loss and corresponding persistence of sorbed contaminants. To improve our ability to predict the fate of contaminants sorbed to the broad spectrum of coloured microplastics in the environment, therefore, we investigated the photodegradation (UVA light,  $\lambda_{\text{max}} = 350$  nm) of the model organic contaminant anthracene sorbed to four coloured polyethylene microplastics. Anthracene loss kinetics were colour dependent (unpigmented  $\gg$  orange  $>$  blue = white), which we attribute to differences in the pigment light absorption profiles for the different microplastics. The findings presented here highlight the need to consider the influence of microplastic pigmentation when evaluating the potential environmental impacts of their associated contaminants.

## 1 Introduction

Microplastics (<5 mm in one dimension) are ubiquitously present in water, soil, air, and organisms.<sup>1,2</sup> In aquatic environments, they accumulate toxic hydrophobic organic contaminants<sup>3,4</sup> and suppress the photodegradative loss of these contaminants.<sup>5-8</sup> As a result, contaminant concentrations sorbed to microplastics are orders of magnitude greater than those in the surrounding water.<sup>4</sup> Thus, in addition to the many direct adverse health outcomes linked to microplastic ingestion,<sup>9</sup> microplastics may act as vectors for organic contaminant uptake by aquatic organisms and transport to remote regions.<sup>10,11</sup>

As plastic products are often coloured for aesthetic and practical reasons, their degradation in the environment results

### Environmental significance

Aquatic microplastics accumulate toxic contaminants, thus facilitating contaminant uptake by aquatic organisms and transport to remote regions. Adequately assessing the importance of these pathways requires us to understand the processes that govern the concentration of sorbed contaminants, such as photodegradation. Although microplastics come in many colours, studies examining the role of microplastic properties and environmental conditions on contaminant photodegradation kinetics have used solely unpigmented microplastics. Here, we show for the first time that the microplastic colour alters contaminant photodegradation kinetics. Our results highlight the urgent need for studies that better represent the colour diversity of the microplastic population to better inform environmental assessments.

in a correspondingly broad spectrum of coloured microplastics.<sup>12-14</sup> For example, a survey classifying the colour of plastic particles (20  $\mu\text{m}$  to 15 cm) collected at the surface of the world's oceans found that they were 31% white, 28% yellow-brown-orange, 16% transparent, 11% blue-green, 7% black, and 2% red.<sup>12</sup> This presence of pigments has been linked to differences in environmental photoaging of plastics, as characterized by changes in their chemical, physical and mechanical properties.<sup>15-18</sup> We hypothesized that microplastic colour may play a similarly key role in the photodegradation of sorbed contaminants, for example by shielding contaminants from direct photodegradation or initiating indirect photodegradation. However, because studies to date have only used unpigmented microplastics, the influence of microplastic colour on contaminant fate remains unknown.

In this study, we show for the first time the influence of microplastic colour on the photodegradation of sorbed contaminants using polyethylene microplastics of four common colours (unpigmented, white, blue, and orange) that would display different light absorption profiles and using the model contaminant anthracene (a combustion product found in aqueous environments and sorbed to microplastics<sup>3,19</sup>). We used polyethylene microplastics here as they are one of the most abundant polymer types found in the environment<sup>9</sup> and, owing

Department of Chemistry & Chemical Biology, McMaster University, Hamilton, L8S 4M1, Canada. E-mail: [stylers@mcmaster.ca](mailto:stylers@mcmaster.ca)



to their density (0.89–0.98 g cm<sup>−3</sup>),<sup>20</sup> are typically located near the water surface<sup>21</sup> where they are exposed to incoming sunlight. We highlight the relationship of anthracene photodegradation kinetics with the microplastic light absorption profiles and discuss the potential implications of this relationship for the environmental fate of microplastic-associated contaminants.

## 2 Materials and methods

### 2.1 Microplastic sourcing and characterization

Polyethylene microspheres (500–600 µm diameter) of different colours (clear (*i.e.*, unpigmented), white, blue, and orange) were obtained from Cospheric. According to the manufacturer, the four microsphere samples were made from the same polyethylene material, and the only compositional difference is the presence of coloured additives in the white, blue, and orange microspheres. The clear microspheres have a density of 0.96–0.98 g cm<sup>−3</sup> (specified as low-density polyethylene), whereas the other three have densities of 1.00 g cm<sup>−3</sup>. Their appearances are shown in Fig. S1. Crystalline phases present in the microspheres were identified using X-ray diffraction (XRD). Patterns were collected using a Bruker D8 Discover instrument with a Cu K $\alpha$  sealed tube radiation source ( $\lambda_{\text{avg}} = 1.54184 \text{ \AA}$ ). The scan had a  $2\theta$  range of 2–100° and 6 frames were collected with an exposure time of 300 s per frame. Absorption profiles (250–800 nm) of the microspheres were obtained using a Cary series UV-vis-NIR spectrophotometer (Agilent Technologies) with a Praying Mantis diffuse reflectance accessory (Harrick Scientific Products). The profiles were scaled to reference spectra obtained for the empty cell (100% transmittance) and a certified reflectance standard (0% transmittance; PTFE Spectralon® disk from Labsphere).

### 2.2 Sorption of anthracene onto the microplastics

Sorption of anthracene onto the microspheres was accomplished by adding microspheres (0.2 g) to an aqueous anthracene solution (10 mL, 30 µg L<sup>−1</sup> in HPLC-grade water) in amber glass vials (12 mL). The total sorption time was 22.5 h, including shaking (500 rpm, IKA® Vibrax VXR) at the beginning (5 h) and end (30 min) of the sorption period. Control experiments with no microspheres showed no anthracene loss (*e.g.*, *via* sorption to the vial walls or evaporation) over the sorption time. After sorption, microsphere samples were vacuum filtered (30 mL fritted glass filter, medium frit) until dry ( $\sim$ 5 min) and used for experiments on the same day. The final concentrations of anthracene sorbed onto the microspheres, as determined *via* extraction of unilluminated samples (see the SI Text S1 for calculation details), were  $587 \pm 80 \text{ ng g}^{-1}$  for unpigmented,  $664 \pm 75 \text{ ng g}^{-1}$  for white,  $696 \pm 102 \text{ ng g}^{-1}$  for blue, and  $573 \pm 68 \text{ ng g}^{-1}$  for orange microspheres (average  $\pm$  one standard deviation of seven trials). While these values are similar, a statistically significant difference ( $p < 0.05$ ) does exist between the clear *vs.* blue, orange *vs.* blue, and orange *vs.* white microspheres. These values are also in the mid-range of typical polycyclic aromatic hydrocarbon (PAH; the class of compounds that

includes anthracene) concentrations measured in microplastics collected from beaches and aquatic environments ( $\sim$ 100–2000 ng g<sup>−1</sup>).<sup>22–27</sup>

### 2.3 Photodegradation experiments

Aqueous suspensions of anthracene-contaminated microspheres (0.03 g,  $\sim$ 345 microspheres, in 4 mL HPLC-grade water) were prepared in borosilicate test tubes (13 × 100 mm, ESBE Scientific); given polyethylene's density, the microspheres floated at the surface in a single layer. These suspensions were then illuminated for 0, 15, 30, 60, 120, or 240 min ( $n = 3$  test tubes for each timepoint) using a Rayonet photoreactor equipped with six UVA lamps ( $\lambda_{\text{max}} = 350 \text{ nm}$ ; Luzchem LZC-355) and a rotating carousel with 12 sample slots. Here, UVA lamps were chosen because their emission spectrum overlaps with anthracene's absorption peaks (Fig. S2). To compare the photodegradation of anthracene when sorbed to microspheres *versus* in water (no microspheres), we also illuminated aqueous solutions of anthracene (4 mL, 15 µg L<sup>−1</sup>) in the same photoreactor for 0, 15, 30, 60, 120, or 240 min ( $n = 3$  test tubes for each timepoint). To quantify the desorption of anthracene from the contaminated microspheres into the clean HPLC-grade water used for the photodegradation experiments and assess its potential contribution to the observed loss upon illumination, we performed a comprehensive set of dark control experiments (see SI Text S2 for related methods).

### 2.4 Quantification of anthracene concentrations

Anthracene concentrations in aqueous solutions were determined using fluorescence spectrometry ( $\lambda_{\text{excitation}} = 355 \text{ nm}$ ,  $\lambda_{\text{emission}} = 402 \text{ nm}$ ; BioTek Cytation 5 microplate reader with a 24-well black polystyrene microplate) *via* comparison to an external calibration curve prepared with standard solutions in HPLC-grade water (2–15 µg L<sup>−1</sup>). Control experiments confirmed minimal (<10%) loss of anthracene to the polystyrene plate walls over the analysis period (<10 min). The mass of anthracene sorbed to the microspheres was determined by isolating the illuminated microspheres *via* vacuum filtration (15 mL fritted glass filter, medium frit) until dry ( $\sim$ 1 min; smaller mass of microspheres took less time to dry than after the bulk sorption step) and extracting the anthracene using acetone (3.5 mL in 12 mL amber glass vials). The total extraction time was 24 h, including shaking (400 rpm) at the beginning (30 min) and end (2 h) of the extraction period. As acetone is incompatible with the polystyrene microplates available for the microplate reader, anthracene concentrations in the acetone extracts were determined using a single cuvette spectrophotometer ( $\lambda_{\text{excitation}} = 355 \text{ nm}$ ,  $\lambda_{\text{emission}} = 402 \text{ nm}$ ; Cary Eclipse fluorescence spectrophotometer with 1 cm quartz cuvettes) *via* comparison to an external calibration curve prepared with standard solutions in acetone (1.5–7.5 µg L<sup>−1</sup>).

### 2.5 Chemicals

Anthracene (200 000 µg L<sup>−1</sup> in methanol), HPLC-grade acetone ( $\geq$ 99.9%), HPLC-grade methanol ( $\geq$ 99.9%), and HPLC-grade water were obtained from Sigma-Aldrich. The anthracene



standard was diluted in methanol to make a  $2500 \mu\text{g L}^{-1}$  stock solution, which was used to make all other aqueous and acetone anthracene solutions. All chemicals were used as received.

### 3 Results and discussion

#### 3.1 Photodegradation of anthracene sorbed to unpigmented versus pigmented microspheres

As illustrated in Fig. 1, anthracene loss kinetics upon illumination exhibit a distinct dependence on microsphere colour (unpigmented  $\gg$  orange  $>$  blue = white). For all microsphere types, the data are well-fit by a single exponential (see Table S1 for all fit parameters), which implies first-order loss kinetics for anthracene when sorbed to microplastics. The rate uncertainties reported below represent one standard deviation of the fits as provided by the curve fitting tool in Igor Pro (version 9.05). The loss rate constant of anthracene sorbed to the unpigmented translucent microspheres ( $0.027 \pm 0.003 \text{ min}^{-1}$ ) is similar to the loss rate constant of anthracene in the aqueous phase ( $0.0272 \pm 0.0006 \text{ min}^{-1}$ ). On the other hand, a suppression ( $1.5\text{--}2.3\times$ ) in anthracene loss kinetics is observed for the three pigmented opaque microspheres ( $0.018 \pm 0.002 \text{ min}^{-1}$  for orange,  $0.012 \pm 0.002 \text{ min}^{-1}$  for blue, and  $0.012 \pm 0.002 \text{ min}^{-1}$  for white). In principle, because aqueous-phase photodegradation of anthracene is rapid, these differences could arise not only from differences in photodegradation loss kinetics of sorbed anthracene but also from differences in anthracene desorption kinetics. In other words, if desorption followed by rapid aqueous-phase photodegradation maintained a concentration gradient between the microspheres and surrounding water that promoted sustained desorption, this would result in desorption rate-limited anthracene loss

kinetics. However, as we show experimentally in the SI (Text S2), anthracene desorption was minimal under our experimental conditions. Therefore, as we discuss in the following paragraphs, we attribute the observed colour dependence to differences in the microplastic-sorbed anthracene photodegradation rates arising from differences in microsphere light absorption profiles.

The overall photodegradation rate of microplastic-sorbed anthracene will depend on the light fluxes experienced by its near-surface and internally diffused fractions, which in turn will be influenced by anthracene's intraparticle diffusion coefficient<sup>28</sup> and the extent of light penetration into the microplastic bulk. As all of the microspheres were made from the same polyethylene material, we would expect the distribution of anthracene within the plastics to be similar; however, as highlighted by the microsphere absorption profiles (Fig. 2), the unpigmented sample absorbs much less light than the pigmented ones over the wavelength range of the UVA lamps ( $\sim 300\text{--}400 \text{ nm}$ ). Thus, we expect light to penetrate deeper into the unpigmented microspheres than the pigmented ones, resulting in the photodegradation of a greater fraction of anthracene. This is further supported by the fact that the photodegradation of anthracene is almost identical when sorbed to the unpigmented microspheres as compared to in the aqueous phase, suggesting that the majority of sorbed anthracene is exposed to the incoming light.

Contrarywise, for the strongly absorbing pigmented microspheres, we expect a greater degree of light shielding, especially for the internal anthracene fraction. Consequently, to photodegrade, this internal fraction would first need to diffuse back toward the surface of the microsphere, with this process being driven by the anthracene concentration gradient within the microsphere resulting from photodegradation of near-surface anthracene. Accordingly, the slower photodegradation kinetics observed for the pigmented microspheres as compared to the unpigmented ones imply that this diffusion step is rate-limiting. Empirical support for this interpretation is provided by the kinetic fits for the pigmented microspheres: in particular,

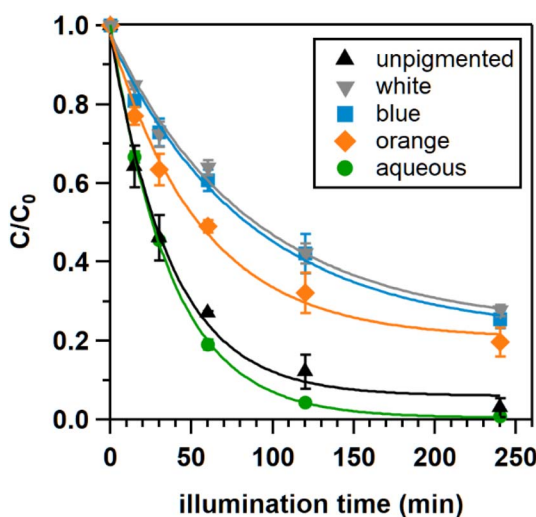


Fig. 1 Photodegradation of anthracene sorbed to unpigmented and pigmented (white, blue, and orange) polyethylene microspheres ( $\sim 600 \text{ ng g}^{-1}$ ). The loss of anthracene in aqueous solution ( $15 \mu\text{g L}^{-1}$ ) is also shown for comparison. Each photodegradation time point represents the average of three separate trials and the error bars are the associated standard deviations; in some cases, these are too small to see. All data were fitted to a single exponential.

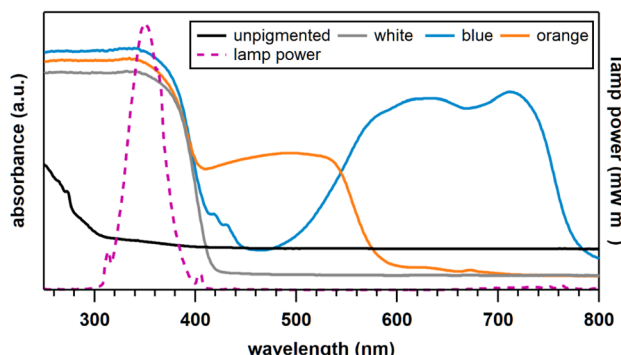


Fig. 2 Absorbance profiles of the unpigmented, white, blue, and orange polyethylene microspheres. Note that the absolute values partially depend on sample packing in the holder, so small observed differences may not represent actual differences in sample absorbance. Overlaid on top is the emission spectrum for the UVA lamps used (provided by Luzchem).



all include large offset values ( $y_0 = \sim 0.2$ , Table S1), which suggests the existence of a second, slower, rate constant associated with anthracene diffusion to the microsphere surface. This type of multi-rate-constant behaviour has been observed previously for PAHs sorbed to soot and fly ash, where the loss kinetics were governed by both surface photodegradation and internal-to-surface diffusion.<sup>29,30</sup>

### 3.2 Photodegradation of anthracene sorbed to different pigmented microspheres

For the three pigmented microspheres studied here, anthracene photodegrades faster ( $\sim 1.5 \times$ ) when sorbed to the orange microspheres than when sorbed to the blue or white ones (Fig. 1 and Table S1). Since all three microspheres absorb strongly in the UVA lamp region (Fig. 2), this suggests that differences in overall light shielding do not account for the different loss rates for the pigmented samples. We attribute this large and similar UVA light absorption to titanium dioxide, a strong UV light absorber present in the pigmented microspheres but not the unpigmented microspheres (see XRD patterns in Fig. S3). This absorption behaviour is not specific to the microspheres used in these experiments but rather would be relevant to many commercial plastics, as titanium dioxide is both the most common white pigment and used extensively in coloured plastics to improve brightness and tinting strength.<sup>31,32</sup>

Although overall light absorption in the UVA region does not differ between pigmented samples, it does differ in the visible region, where the pigments absorb the complementary wavelengths to the sample colour (Fig. 2). In the case of the orange microspheres, this means that the orange pigment peak is in the blue and near-UV region (ending  $\sim 580$  nm). Assuming that this peak is similarly broad to the blue pigment absorption peak (at  $\sim 500$ – $800$  nm), we would expect the tail of the orange pigment peak at the lower wavelength end to partially overlap with the UVA lamp wavelengths. Thus, the faster loss rates we see for orange could reflect absorption of UVA light by the orange pigment, which could lead to the generation of reactive species (e.g., singlet oxygen, hydroxyl radical) and thereby initiate the indirect photodegradation of anthracene.

As all peaks in the microsphere XRD patterns were assignable to either polyethylene or titanium dioxide (Fig. S3), we can conclude that the orange pigment is not a common crystalline colourant (e.g., metal oxides or sulfides)<sup>33–35</sup> but instead is non-crystalline. For example, organic pigments are commonly used to colour orange plastics (e.g., *trans*-perinone or substituted benzimidazolone azo pigments).<sup>36,37</sup> Similarly structured organic orange dyes (aryl azo naphthol dyes) have been shown to photogenerate singlet oxygen,<sup>38</sup> which is known to react with anthracene resulting in indirect photodegradation.<sup>39</sup> However, since the manufacturer did not specify the pigments used in the orange or blue microspheres, we cannot conclusively say that indirect photodegradation is occurring and, if it is, the exact indirect pathway.

For all pigmented samples, we cannot discount indirect photodegradation contributions from titanium dioxide itself, which upon absorption of light generates an electron–hole pair

that can donate or accept electrons to form reactive species such as singlet oxygen or hydroxyl radical.<sup>32</sup> If this titanium dioxide-mediated indirect photodegradation is occurring, we can assume that it would be similar for all three pigmented samples and therefore may be partially masking the influences of light shielding on the kinetics. Thus, the differences in rates for the direct photodegradation of anthracene (*i.e.*, controlled primarily by light penetration) could be even larger for pigmented *versus* unpigmented samples than the total rates (*i.e.*, combined direct and indirect photodegradation) reported here. The importance of this potential masking is unclear, though, since titanium dioxide pigments are often coated with silica or alumina to reduce its photoactivity<sup>32,40</sup> and, in our samples, the titanium dioxide is present as rutile, one of its less photoactive polymorphs.<sup>41</sup>

Here, we explained the observed dependence of anthracene photodegradation kinetics on microsphere colour in relation to their different light absorption profiles. Another possibility that we cannot exclude is the potential influence of pigments on other microsphere properties (*e.g.*, porosity, surface area, surface charge) and resulting anthracene photodegradation kinetics. However, since all microspheres were made from the same polyethylene material and have the same size range, we expect these property differences to be minimal and the interaction of the pigments with light to be the most important difference in relation to contaminant photodegradation.

### 3.3 Environmental significance

We show here that the photodegradation kinetics of microplastic-sorbed anthracene vary with microsphere colour. Based on the rates determined for our experimental conditions, we would expect that anthracene will be more persistent when sorbed to opaque pigmented microplastics compared to translucent unpigmented ones. This suggests that opaque microplastics may be more important vectors for anthracene ingestion by aquatic organisms and transport to remote regions. Additionally, we would expect anthracene to be more persistent when sorbed to blue or white microplastics than when sorbed to orange microplastics.

Our experiments were conducted under simplified conditions (*i.e.*, one contaminant, anthracene, in HPLC grade water) as a first step towards assessing the influence of microplastic colour. However, other microplastic-sorbed contaminants may absorb light differently, react by different pathways, and thus be influenced by the presence of pigments in different ways. Furthermore, under real-world conditions, the relative persistence of contaminants on different coloured microplastics may be influenced by additional microplastic-specific (*e.g.*, biofilm formation, microplastic age) or environmental (*e.g.*, water composition) factors. While the effects of these factors on contaminant photodegradation has been investigated for unpigmented microplastics,<sup>7,42–44</sup> the combined effects of these factors with microplastic pigmentation remains unknown. For example, microplastic aging can lead to pigment degradation and colour fading,<sup>15</sup> which would change both the microplastic light absorption profile and its potential to generate reactive



oxygen species, thereby altering the photodegradation kinetics of sorbed contaminants. Thus, more work using coloured microplastics is needed to accurately predict the impact of colour on sorbed contaminant lifetime, and our results serve as a call to action and foundation for the design of such studies.

## 4 Conclusion

Microplastic colour is an important but overlooked influence on the photodegradation of microplastic-sorbed contaminants and may control the relative abundance of contaminants on different coloured microplastics. These differences may be important for ecosystem health, as the probability that organisms will ingest a certain microplastic colour and its varying levels of associated contaminants depends both on the relative abundances of each colour and the feeding habits of each specific organism. For example, the contribution of unpigmented microplastics to overall microplastic loadings was much larger in a Chinese river (37%)<sup>14</sup> than off the coast of India (10%),<sup>13</sup> whereas the relative abundance of blue microplastics was similar in both locations (~20%). In addition, studies have suggested that organisms will preferentially ingest microplastics with colours similar to their food sources: for example, goldfish preferentially ingested black and green microplastics,<sup>45</sup> while Amberstripe scad preferentially ingested blue microplastics.<sup>46</sup> Understanding the interplay of microplastic colour abundances, ingestion rates, and contaminant persistence will therefore be crucial to evaluating the impact of microplastic-contaminant systems on aquatic organisms and informing potential future guidelines for plastic pigment usage.

## Author contributions

L. C. M. developed the methods, conducted experiments, analyzed the data, and wrote the manuscript with guidance and critical comments from S. A. S.

## Conflicts of interest

There are no conflicts to declare.

## Data availability

The data supporting this article have been included as part of the SI ("Supplementary data.xlsx").

The supplementary information pdf contains the following: procedure for determining the amount of anthracene sorbed to the microspheres (Text S1); methods and results for the dark experiments assessing the potential contribution of anthracene desorption (Text S2). Physical appearance of the microspheres (Fig. S1); emission spectrum of the UVA lamps and absorption spectrum of anthracene (Fig. S2); XRD patterns of the microspheres (Fig. S3); consecutive dark cycle experiments to assess desorption (Fig. S4); rate constants and additional fit parameters (Table S1); comparison of anthracene loss after 15 and 30 min for dark or illuminated experiments (Table S2). See DOI: <https://doi.org/10.1039/d5em00529a>.

## Acknowledgements

This research was undertaken, in part, thanks to funding from the Canada Research Chairs program. The authors acknowledge the Department of Chemistry & Chemical Biology and the Faculty of Science at McMaster University for start-up funding and the Natural Sciences and Engineering Research Council of Canada (NSERC) for funding through the Discovery Grants Program. We thank the Canada Foundation for Innovation (CFI) and the Ontario Research Fund – Research Infrastructure for funding through the John R. Evans Leaders Fund and Small Infrastructure Fund programs. We thank Daniel Hrabowij and Dr Alex Adronov for assistance with the UV-vis absorbance analysis, Suha Saleem and Victoria Jarvis for performing the XRD analysis, Dr Ryan Wylie for use of his microplate reader, Julie Gauthier for use of the fluorescence spectrophotometer, and Dr Willie Leigh for the donation of the photoreactor used in these experiments (all from McMaster University). We recognize and acknowledge that McMaster University is located on the traditional territories of the Mississauga and Haudenosaunee nations, and within the lands protected by the Dish with One Spoon wampum agreement.

## References

- 1 J. Peng, J. Wang and L. Cai, Current understanding of microplastics in the environment: Occurrence, fate, risks, and what we should do, *Integr. Environ. Assess. Manage.*, 2017, **13**, 476–482.
- 2 P. Roy, A. K. Mohanty and M. Misra, Microplastics in ecosystems: their implications and mitigation pathways, *Environ. Sci.: Adv.*, 2022, **1**, 9–29.
- 3 W. Mei, G. Chen, J. Bao, M. Song, Y. Li and C. Luo, Interactions between microplastics and organic compounds in aquatic environments: A mini review, *Sci. Total Environ.*, 2020, **736**, 139472.
- 4 I. A. O'Connor, L. Golsteijn and A. J. Hendriks, Review of the partitioning of chemicals into different plastics: Consequences for the risk assessment of marine plastic debris, *Mar. Pollut. Bull.*, 2016, **113**, 17–24.
- 5 K. Noro and Y. Yabuki, Photolysis of polycyclic aromatic hydrocarbons adsorbed on polyethylene microplastics, *Mar. Pollut. Bull.*, 2021, **169**, 112561.
- 6 K. Noro, Y. Kakimoto, Q. Wang, S. Akiyama, T. Takikawa, R. Omagari, Y. Yabuki and T. Amagai, Enhancement of photodegradation of polyethylene with adsorbed polycyclic aromatic hydrocarbons under artificial sunlight irradiation, *Mar. Pollut. Bull.*, 2023, **194**, 115331.
- 7 L. Yin, S. Zhang, B. Liu, Q. Zheng, Z. Wang and R. Qu, Investigation of the photolysis process of benzo(a)anthracene (BaA) on polyvinyl chloride (PVC) and polystyrene (PS) microplastics: Plastics aging effect, transformation products and toxicity assessment, *Sci. Total Environ.*, 2024, **929**, 172394.
- 8 C. Chen, L. Chen, Y. Li, W. Fu, X. Shi, J. Duan and W. Zhang, Impacts of microplastics on organotins' photodegradation in aquatic environments, *Environ. Pollut.*, 2020, **267**, 115686.



9 M. Ateia, G. Ersan, M. G. Alalm, D. C. Boffito and T. Karanfil, Emerging investigator series: microplastic sources, fate, toxicity, detection, and interactions with micropollutants in aquatic ecosystems – a review of reviews, *Environ. Sci.: Processes Impacts*, 2022, **24**, 172–195.

10 N. B. Hartmann, S. Rist, J. Bodin, L. H. S. Jensen, S. N. Schmidt, P. Mayer, A. Meibom and A. Baun, Microplastics as vectors for environmental contaminants: Exploring sorption, desorption, and transfer to biota, *Integr. Environ. Assess. Manage.*, 2017, **13**, 488–493.

11 L. M. Ziccardi, A. Edgington, K. Hentz, K. J. Kulacki and S. K. Driscoll, Microplastics as vectors for bioaccumulation of hydrophobic organic chemicals in the marine environment: A state-of-the-science review, *Environ. Toxicol. Chem.*, 2016, **35**, 1667–1676.

12 E. Martí, C. Martin, M. Galli, F. Echevarría, C. M. Duarte and A. Cázar, The colors of the ocean plastics, *Environ. Sci. Technol.*, 2020, **54**, 6594–6601.

13 K. Patidar, B. Ambade and M. Alshehri, Microplastics and associated polycyclic aromatic hydrocarbons in surface water and sediment of the Bay of Bengal coastal area, India: sources, pathway and ecological risk, *Environ. Geochem. Health*, 2024, **46**, 176.

14 Y. Mai, S. Peng, Z. Lai and X. Wang, Measurement, quantification, and potential risk of microplastics in the mainstream of the Pearl River (Xijiang River) and its estuary, Southern China, *Environ. Sci. Pollut. Res.*, 2021, **28**, 53127–53140.

15 J. Su, J. Ruan, D. Luo, J. Wang, Z. Huang, X. Yang, Y. Zhang, Q. Zeng, Y. Li, W. Huang, L. Cui and C. Chen, Differential photoaging effects on colored nanoplastics in aquatic environments: Physicochemical properties and aggregation kinetics, *Environ. Sci. Technol.*, 2023, **57**, 15656–15666.

16 S. Key, P. G. Ryan, S. E. Gabbott, J. Allen and A. P. Abbott, Influence of colourants on environmental degradation of plastic litter, *Environ. Pollut.*, 2024, **347**, 123701.

17 X. Li, D. Huang, H. Dong, J. Wen, J. Dong, C. Zhang, L. Li and H. Zhang, Differential photoaging behaviors of different colored commercial polyethylene microplastics in water: The important role of color characteristics, *Sci. Total Environ.*, 2024, **956**, 177361.

18 A. J. Robinson, J. Wray and D. A. Worsley, Effect of coloured pigmentation on titanium dioxide photo catalysed PVC degradation, *Mater. Sci. Technol.*, 2006, **22**, 1503–1508.

19 A. Mojiri, J. L. Zhou, A. Ohashi, N. Ozaki and T. Kindaichi, Comprehensive review of polycyclic aromatic hydrocarbons in water sources, their effects and treatments, *Sci. Total Environ.*, 2019, **696**, 133971.

20 M. Kooi and A. A. Koelmans, Simplifying microplastic via continuous probability distributions for size, shape, and density, *Environ. Sci. Technol. Lett.*, 2019, **6**, 551–557.

21 P. L. Lenaker, A. K. Baldwin, S. R. Corsi, S. A. Mason, P. C. Reneau and J. W. Scott, Vertical distribution of microplastics in the water column and surficial sediment from the Milwaukee River Basin to Lake Michigan, *Environ. Sci. Technol.*, 2019, **53**, 12227–12237.

22 C. M. Rochman, E. Hoh, B. T. Hentschel and S. Kaye, Long-term field measurement of sorption of organic contaminants to five types of plastic pellets: Implications for plastic marine debris, *Environ. Sci. Technol.*, 2013, **47**, 1646–1654.

23 J. C. Antunes, J. G. L. Frias, A. C. Micaelo and P. Sobral, Resin pellets from beaches of the Portuguese coast and adsorbed persistent organic pollutants, *Estuarine, Coastal Shelf Sci.*, 2013, **130**, 62–69.

24 O. H. Fred-Ahmadu, I. T. Tenebe, O. O. Ayejuo and N. U. Benson, Microplastics and associated organic pollutants in beach sediments from the Gulf of Guinea (SE Atlantic) coastal ecosystems, *Chemosphere*, 2022, **298**, 134193.

25 J. P. G. L. Frias, P. Sobral and A. M. Ferreira, Organic pollutants in microplastics from two beaches of the Portuguese coast, *Mar. Pollut. Bull.*, 2010, **60**, 1988–1992.

26 L. M. Rios, C. Moore and P. R. Jones, Persistent organic pollutants carried by synthetic polymers in the ocean environment, *Mar. Pollut. Bull.*, 2007, **54**, 1230–1237.

27 W. Zhang, X. Ma, Z. Zhang, Y. Wang, J. Wang, J. Wang and D. Ma, Persistent organic pollutants carried on plastic resin pellets from two beaches in China, *Mar. Pollut. Bull.*, 2015, **99**, 28–34.

28 E. Fries and C. Zarfl, Sorption of polycyclic aromatic hydrocarbons (PAHs) to low and high density polyethylene (PE), *Environ. Sci. Pollut. Res.*, 2012, **19**, 1296–1304.

29 D. Kim, T. M. Young and C. Anastasio, Phototransformation rate constants of PAHs associated with soot particles, *Sci. Total Environ.*, 2013, **443**, 896–903.

30 J. Niu, P. Sun and K.-W. Schramm, Photolysis of polycyclic aromatic hydrocarbons associated with fly ash particles under simulated sunlight irradiation, *J. Photochem. Photobiol. A*, 2007, **186**, 93–98.

31 A. Turner and M. Filella, The role of titanium dioxide on the behaviour and fate of plastics in the aquatic environment, *Sci. Total Environ.*, 2023, **869**, 161727.

32 R. E. Day, The role of titanium dioxide pigments in the degradation and stabilisation of polymers in the plastics industry, *Polym. Degrad. Stab.*, 1990, **29**, 73–92.

33 G. Pfaff, Iron oxide pigments, *Phys. Sci. Rev.*, 2021, **6**, 535–548.

34 G. Pfaff, Cerium sulfide pigments, *Phys. Sci. Rev.*, 2022, **7**, 45–48.

35 G. Pfaff, Mixed metal oxide pigments, *Phys. Sci. Rev.*, 2022, **7**, 7–16.

36 R. Christie and A. Abel, Perylene and perinone pigments, *Phys. Sci. Rev.*, 2021, **6**, 569–580.

37 R. Christie and A. Abel, Monoazo (Monohydrazone) pigments based on benzimidazolones, *Phys. Sci. Rev.*, 2022, **7**, 17–30.

38 F. Ruyffelaere, V. Nardello, R. Schmidt and J.-M. Aubry, Photosensitizing properties and reactivity of aryl azo naphthol dyes towards singlet oxygen, *J. Photochem. Photobiol. A*, 2006, **183**, 98–105.

39 J. N. Grossman, S. F. Kowal, A. D. Stubbs, C. N. Cawley and T. F. Kahan, Anthracene and pyrene photooxidation



kinetics in saltwater environments, *ACS Earth Space Chem.*, 2019, **3**, 2695–2703.

40 D. A. Worsley and J. R. Searle, Photoactivity test for  $TiO_2$  pigment photocatalysed polymer degradation, *Mater. Sci. Technol.*, 2002, **18**, 681–684.

41 J. Zhang, P. Zhou, J. Liu and J. Yu, New understanding of the difference of photocatalytic activity among anatase, rutile and brookite  $TiO_2$ , *Phys. Chem. Chem. Phys.*, 2014, **16**, 20382–20386.

42 L. Yin, N. Wu, R. Qu, F. Zhu, J. S. Ajarem, A. A. Allam, Z. Wang and Z. Huo, Insight into the photodegradation and universal interactive products of 2,2',4,4'-tetrabromodiphenyl ether on three microplastics, *J. Hazard. Mater.*, 2023, **445**, 130475.

43 Z. Wang, Y. Zhai, G. Liu, X. Liu, X. Liu, Y. Zhou, C. Huang, W. Wang and M. Xu, Effect of polystyrene microplastics on tetracycline photoconversion under simulated sunlight: Vital role of aged polystyrene, *Sci. Total Environ.*, 2023, **897**, 165399.

44 N. Wu, W. Cao, R. Qu, D. Zhou, C. Sun and Z. Wang, Photochemical transformation of decachlorobiphenyl (PCB-209) on the surface of microplastics in aqueous solution, *Chem. Eng. J.*, 2021, **420**, 129813.

45 X. Xiong, Y. Tu, X. Chen, X. Jiang, H. Shi, C. Wu and J. J. Elser, Ingestion and egestion of polyethylene microplastics by goldfish (*Carassius auratus*): influence of color and morphological features, *Helijon*, 2019, **5**, e03063.

46 N. C. Ory, P. Sobral, J. L. Ferreira and M. Thiel, Amberstripe scad *Decapterus muroadsi* (Carangidae) fish ingest blue microplastics resembling their copepod prey along the coast of Rapa Nui (Easter Island) in the South Pacific subtropical gyre, *Sci. Total Environ.*, 2017, **586**, 430–437.

